INTERNATIONAL ATOMIC ENERGY AGENCY
UNITED NATIONS EDUCATIONAL, SCIENTIFIC AND CULTURAL ORGANIZATION
INTERNATIONAL CENTRE FOR THEORETICAL PHYSICS
I.C.T.P., P.O. BOX 586, 34100 TRIESTE, ITALY. CABLE CENTRATOM TRIESTE

H4.SMR/782-17

Second Workshop on
Three-Dimensional Modelling of Seismic Waves
Generation, Propagation and their Inversion

7 - 18 November 1994

Peculiarities of Surface-Wave Propagation Across Central Eurasia

A. Levshin - L. Ratnikova

University of Colorado
Department of Physics
Boulder, Colorado
U.S.A.

Bulletin of the Seismological Society of America, Vol. 82, No. 6, 2464–2493, December 1992

PECULIARITIES OF SURFACE-WAVE PROPAGATION ACROSS CENTRAL EURASIA

By Anatoli Levshin, Ludmila Ratnikova, and Jon Berger

Abstract

The recent installation of six broadband digital IRIS / IDA seismic stations in the USSR has provided new opportunities for studying surface-wave propagation across Eurasia. Group velocities of fundamental Rayleigh and Love modes between epicenters and these stations were determined for 35 events that occurred since April 1989 to the middle of July 1990 near Eurasia. Differential phase velocities were found for the same arrivals along paths between several pairs of stations. Group and phase velocities were obtained in the period range from 15 to 300 sec. Frequency-time polarization analysis was used for studying polarization properties of surface waves. In some cases, significant anomalies in the particle motion for periods up to 100 sec were observed. They are attributed to surface-wave refraction and scattering due to lateral inhomogeneities at the boundaries and inside the Eurasia continent.

Introduction

Numerous studies of the deep structure of the central Eurasia lithosphere have been undertaken during the second half of this century. Most of them were based on *P*-wave travel times from earthquakes to seismic stations inside and around this region (Louck and Nersesov, 1965; Alekseev *et al.*, 1973; Bougaevskii, 1978). In recent years, several deep seismic sounding profiles, some of them more than 3000-km long, crossed the continent. These have provided detailed information about the *P*-velocity cross section of the crust and upper mantle (Volvovsky, 1973; Volvovsky and Volvovsky, 1975; Belyaevsky *et al.*, 1977; Ryaboy, 1979; Vinnik and Egorkin, 1980; Vinnik and Ryaboy, 1981; Egorkin and Pavlenkova, 1981; Antonenko, 1984; Egorkin *et al.*, 1984; Zunnunov, 1985). Shear-velocity structure of the same area is not so well determined. As shear waves are more sensitive to partial melting, crystal aligning, non-hydrostatic stresses of the mantle material than *P* waves, the knowledge of the *S*-velocity structure of this huge region is very essential for further progress in understanding tectonic evolution of Eurasia. Several studies to recover this information from surface-wave recordings have been done (Knopoff and Chang, 1976; Chang, 1979; Patton, 1980; Liao, 1981; Levshin *et al.*, 1982; Barmin *et al.*, 1984; Kozhevnikov, 1987; Kozhevnikov and Barmin, 1989). Unfortunately, the absence of broadband seismic stations inside this area seriously handicapped these studies, limiting their resolving power and depth penetration. The Joint Seismic Studies Program of IRIS (Incorporated Research Institutions for Seismology) and Academy of Sciences of the USSR, undertaken in the framework of the Intergovernmental Agreement on Cooperation in the Field of Environmental Protection, has provided new opportunities for such studies. Several modern broadband digital stations were installed in this area during 1988. Records obtained from these stations in 1989 and 1990 were used to study surface-wave propagation across central Eurasia. The time span of data used in this study

was too short for a statistically supported one-dimensional inversion or a full-scale tomographic inversion of surface-wave velocities or waveforms (Nolet, 1987). The purposes of this paper are (1) to describe some new methods and software for surface-wave processing; and (2) to demonstrate that their application to high-quality digital records permits investigation of some effects of regional lateral inhomogeneities of central Eurasia on surface-wave dispersion and polarization. Such information will be helpful in the future when the amount of data accumulated by these and newly deployed stations are sufficient for structural inversion.

Instruments and Data

The IRIS/IDA-USSR stations sites are shown in Figure 1 and Table 1. Surface-wave data were obtained from continuous records of the IRIS/IDA broadband system. This system uses Streckheisen STS-VBB seismometers and a data logger with a sampling rate of 20 samples per second (Given, 1990). Although the stations were installed only a short time ago, they recorded a number of events with clear surface-wave trains. Two types of events were selected for analysis. The first includes earthquakes that occurred inside Eurasia or along its border so that the wave paths to stations cross the continent and the surface waves are well recorded by at least one of the stations. These events provided us with epicenter-to-station group and phase velocities. The second type includes events that occurred near the great circle passing through any pair of our stations and that were strong enough for surface waves to be well recorded by both stations. We set the condition that azimuths from epicenter to each of the two stations should differ by less than 6°. Events selected in this way provided data for interstation measurements of phase velocities. Epicenters of the selected events are shown in Figure 1; the source parameters of events are given in Table 2.

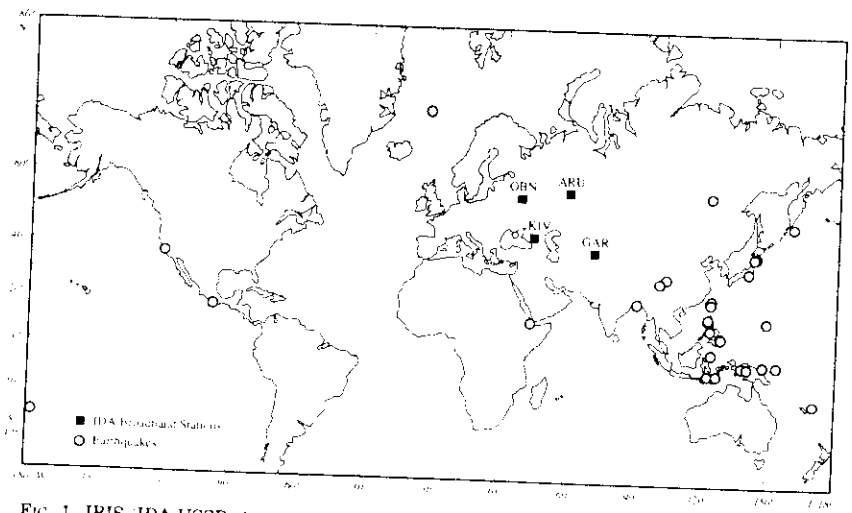

FIG. 1. IRIS/IDA-USSR sites and epicenters of studied events. Stations are shown by squares, epicenters by circles.

TABLE 1

STATION LOCATIONS

STA	Station	North Latitude	East Longitude	Elevation (m)
ARU	Arti	56.40	58.60	250
GAR	Garm	39.10	70.77	1600
KIV	Kislovodsk	43.95	42.68	1300
OBN	Obninsk	55.11	36.57	160

TABLE 2

EVENT LOCATIONS AND PARAMETERS

Date (m/d/y)	Origin Time	Geographic Position	Latitude	Longitude	Depth	Magnitude M_b	Magnitude M_s
04/11/89	20:24:11	Kamchatka	49.48	159.18	33	6.3	6.5
04/15/89	20:34:09	S. W. China	29.98	99.24	33	6.2	6.2
04/20/89	22:59:54	Stanovoy R	57.14	121.92	33	6.0	6.5
04/25/89	14:29:00	Mexico	16.81	−99.38	20	6.3	6.9
05/03/89	05:53:00	S. W. China	30.05	99.48	10	6.0	6.1
05/03/89	15:41:31	S. W. China	30.05	99.49	10	5.9	5.9
05/14/89	00:59:49	Kermadec	−30.55	−178.40	33	5.9	6.6
06/09/89	12:19:35	Norweg. Sea	71.42	−4.67	10	5.5	5.5
06/12/89	04:10:49	Burma	21.86	89.76	10	6.0	5.1
07/14/89	20:42:46	Timor	8.04	125.15	59	6.4	0.0
07/13/89	17:07:30	Timor	−8.03	121.23	33	6.3	6.3
08/03/89	11:31:20	Ryukyu	23.00	122.02	10	5.9	6.3
08/20/89	11:16:56	Djibouti	11.75	41.94	10	5.8	6.3
08/20/89	11:46:27	Djibouti	11.86	41.78	10	6.1	5.7
08/20/89	11:56:17	Djibouti	11.76	41.96	10	5.3	0.0
08/20/89	19:25:56	Djibouti	11.90	41.82	10	6.1	5.6
08/21/89	01:09:05	Djibouti	11.87	41.84	10	6.3	6.2
08/21/89	23:12:41	Ryukyu	24.09	122.50	41	5.6	6.2
09/04/89	05:20:59	N. Guinea	−4.24	136.64	33	5.8	6.1
09/22/89	02:25:54	S. W. China	31.54	102.46	33	6.0	6.1
09/25/89	14:17:50	Loyalty Is	−20.32	169.24	55	6.1	0.0
10/17/89	16:27:53	New Ireland	−4.04	152.40	33	6.0	0.0
10/18/89	00:04:15	N. Californ.	37.04	121.88	18	6.6	7.1
10/29/89	05:25:41	Japan	39.55	141.33	28	6.0	6.0
11/01/89	18:25:35	Japan	39.80	142.84	38	6.3	7.3
12/15/89	18:43:46	Philippines	8.39	126.78	33	6.1	7.4
12/20/89	00:08:25	Philippines	8.13	126.88	64	6.0	0.0
12/30/89	23:18:49	Bismark sea	−3.43	146.13	33	5.6	6.6
02/20/90	06:53:39	Japan	34.69	139.35	13	6.1	6.4
04/05/90	21:12:38	Marian Tr.	15.23	147.53	32	6.5	7.5
04/18/90	13:39:19	Sulawesi	1.16	122.84	28	6.2	7.4
06/14/90	14:07:40	Philippines	11.33	122.17	15	6.0	7.0
07/16/90	07:26:34	Philippines	15.66	121.23	25	6.6	7.8
07/17/90	21:14:41	Philippines	16.40	121.02	7	6.0	6.6

Data Analysis

Techniques used are interactive and computer-oriented, relying on a successive use of the frequency-time representation of signals (Dziewonski *et al.* 1972;

Levshin *et al.*, 1972; see Keilis-Borok, 1989, for details). Broadband records were decimated using the Seismic Analysis Code (SAC) in order to reduce the sampling rate to 1 sample per second. The decimated data were subjected to the frequency-time analysis (FTAN) using a set of narrow-band gaussian filters. As this procedure has some additional features that distinguish it from other similar, routines, we will discuss it in some detail.

FTAN

The first step in implementing FTAN is a specific Fourier transform of a detrended time series into the frequency domain: $w(t) \rightarrow W(\omega)$ and a phase correction $W(\omega) \rightarrow \tilde{W}(\omega)$ for the instrument phase response. The second step is multiple narrowband filtering by the comb of N Gaussian filters:

$$F(\omega - \omega_i) = \exp\left[-\alpha_i\left(\frac{\omega - \omega_i}{\omega_i}\right)^2\right], \quad i = 1, \ldots, N, \tag{1}$$

where ω_i and α_i are parameters governing the central frequency and relative width of filters. The output of the filtering procedures may be considered as a discrete image of complex frequency-time representation of input record, namely

$$S(\omega, t) = \int_{-\infty}^{\infty} \tilde{W}(\lambda) F(\lambda - \omega) \exp(i\lambda t)\, d\lambda. \tag{2}$$

For fixed $\omega = \omega_i$, $|S(\omega_i, t_j)|$ is the envelope and $\arg S(\omega_i, t_j)$ is the temporal phase of the narrowband output of the ith filter. Actually two matrices $|S(\omega_i, t_j)|$ and $\arg S(\omega_i, t_j)$, $i = 1, \ldots, N$; $j = 1, \ldots, M$ are stored, M being the number of points at the filtered outputs. The values of $S(\omega_i, t_j)$ between points of a grid (ω_i, t_j) are found by a spline interpolation. The map of normalized amplitudes $20 \log_{10}(|S(\omega_i, t_j)|/\max_{i,j}|S(\omega_i, t_j)|)$ is displayed on the screen of the terminal. An automated search of group time $t_{gr}(\omega_i)$ corresponding to $\max_t|S(\omega_i, t)|$ for all ω_i is done and group travel-time curve $t_{gr}(\Omega_i)$ is found and displayed above the amplitude map. Here Ω_i is an apparent frequency of the signal defined as

$$\Omega_i = \frac{\partial}{\partial t} \arg S(\omega_i, t)|_{t = t_{gr}(\omega_i)}. \tag{3}$$

Both theoretical considerations and numerical tests have shown that such an estimate of group times is less biased by amplitude spectrum variations than more usual one $t_{gr}(\omega_i)$ (Keilis-Borok, 1989). Then the preliminary group velocity curve $U(\omega) = r/t_{gr}(\omega)$ is obtained, where r is an epicentral distance and $t_{gr}(\omega)$ is obtained by interpolation of $t_{gr}(\Omega_i)$.

Floating Filtering

At this stage, one may apply "floating" filtering to extract desired signal which covers definite region of the frequency-time amplitude map (Cara, 1973; Keilis-Borok, 1989). This operation improves group time and phase estimates. It is implemented using interactive phase equalization technique (Dziewonski *et al.*, 1972) and time windowing. The interpreter draws on the screen the group velocity curve that follows the amplitude ridge of filtered signal within the frequency range (ω_0, ω_1) where the signal is well observed. Then the phase

correction $\psi(\omega)$ is introduced into spectrum $\tilde{W}(\omega)$ by multiplying it by the factor $\exp[i\psi(\omega)]$, where

$$\psi(\omega) = r\int_{\omega_0}^{\omega_1} 1/U(\omega)\, d\omega + c1^*\omega. \tag{4}$$

Here $U(\omega)$ is obtained by a spline interpolation of the curve drawn on the screen, and the constant $c1$ is chosen to compress the signal around the average group time. The inverse Fourier transform of the phase equalized spectrum produces the compressed signal $\hat{w}(t)$. In the absense of noise and other signals, such a compressed waveform would be similar to a δ-function, but in reality some additional oscillations may be present. Then we apply a cosine-tapered window to the displayed envelope of $\hat{w}(t)$ around the distinct impulsive part related to the desired signal. As a result, the selected signal is enhanced due to suppression of random noise and signals that have different dispersion curves. After transforming the tapered signal $\hat{w}(t)$ into the spectrum $W(\omega)$, we restore the initial phase spectrum by multiplying $W(\omega)$ times the factor $\exp[-i\psi(\omega)]$ and finally return to the time domain with a cleaned dispersed signal $w_c(t)$. Now one may apply FTAN once again for more accurate measurements of dispersion parameters. A sequence of such operations is shown in Figure 2 for the OBN record of an event near the Kamchatka coast that occurred on 11 April

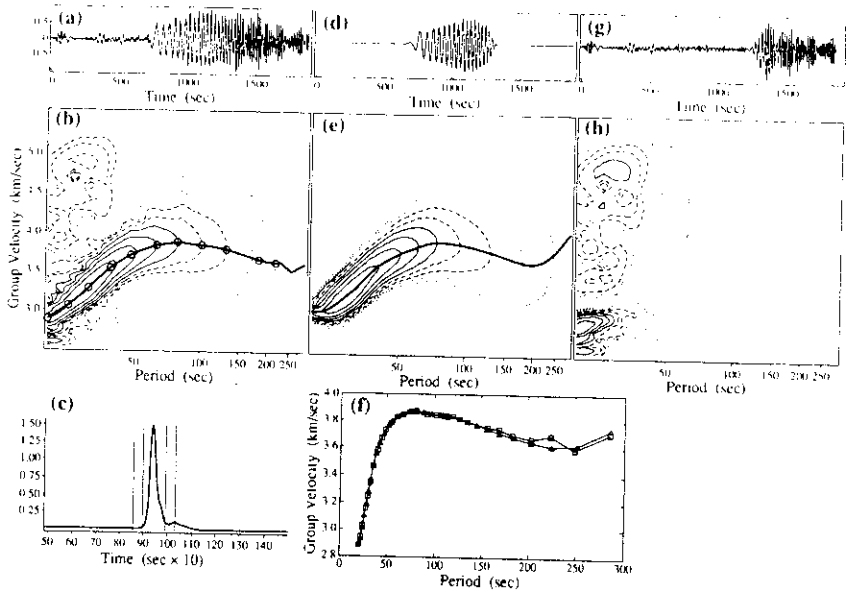

FIG. 2. FTAN of the vertical component seismogram of the station OBN for the event on Kamchatka. (a) Input record. (b) FTAN-diagram of (a). Isolines of the signal power are given with 4-dB increment. Empty circles are set by interpreter on the screen of a terminal along group velocity curve of the main signal. (c) Envelope of the compressed signal. Vertical lines are limits of two tapering windows applied to the compressed signal. (d) Filtered signal. (e) FTAN-diagrams of (d). (f) Group velocity curves from input (squares) and filtered (triangles) signals. (g) Residual seismogram obtained by subtraction of (d) from (a). (h) FTAN-diagram of (g).

1989. Only the vertical component is processed to determine fundamental Rayleigh-mode dispersion over the period range from 20 to 300 sec. The residual record obtained after subtraction of the filtered signal from the original seismogram is shown in Figure 2g. Only strong high-frequency coda and comparatively weak higher modes can be seen in the residual record and the corresponding FTAN diagram shown in Figure 2h.

Differential Phase Velocity Measurements

If we have records from two stations laying near the same great circle with an epicenter at an acceptable distance, we may measure the phase velocity dispersion curve for a path between the stations using the FTAN representations of the two signals. Suppose that we already have the group time curves $t^1_{gr}(\omega)$ and $t^2_{gr}(\omega)$ and the temporal phase estimates $\varphi^1(\omega)$ and $\varphi^2(\omega)$, where $\varphi^k(\omega)$ ($k = 1, 2$) is obtained from discrete values $\varphi^k(\Omega_i)$ by parabolic interpolation and $\varphi^k(\Omega_i)$ is determined by formula

$$\varphi^k(\Omega_i) = \arg S^k(\omega_i, t)|_{t = t_{gr}(\omega_i)}. \tag{5}$$

Then we obtain the following phase velocity estimate

$$C(\omega) = \frac{r_1 - r_2}{t^1_{gr}(\omega) - t^2_{gr}(\omega) - (\varphi^1(\omega) - \varphi^2(\omega) + 2\pi N)/\omega}. \tag{6}$$

Here N is an unknown integer chosen by the condition that $C(\omega)$ be in the prescribed range for some reference low frequency. As an example of such procedure, the phase velocity curve of the fundamental Rayleigh mode is shown in Figure 3 for the path between stations ARU and KIV. The three different curves correspond to FTAN-processing of the unfiltered records, the direct differential phase spectral measurements and FTAN-processing of the filtered records. The last curve is indistinguishable from the curve obtained by direct phase spectral measurements of the filtered records.

Frequency-Time Polarization Analysis (FTPAN)

Polarization analyses are commonly made either in time or frequency domain (e.g., Vidale, 1986; Lerner-Lam and Park, 1989). Interference of different waves overlapping in time or frequency range may seriously distort results of such measurements. It is especially true in the case of surface-wave fields composed of several dispersive modes of Rayleigh and Love waves and their coda. Because surface-wave signals are better resolved in a frequency-time domain, we have applied in this study of polarizational properties of surface-wave technique developed by Lander (in Keilis-Borok, 1989; Paulssen *et al.*, 1990). It is based on vectorial frequency-time representation $\mathbf{S}(\omega, t)$ of three-component record. Each component is processed in the same manner as described above and each value $S_n(\omega, t)$ (n = Z, NS, EW component) is considered as the corresponding component of the vector $\mathbf{S}(\omega, t)$. Then the covariance matrix is calculated using formula

$$\mathbf{C}(\omega) = \frac{\int_{\epsilon(\omega,t)} \mathbf{S}(\Omega,\tau)\mathbf{S}^{T^*}(\Omega,\tau)\, d\Omega\, d\tau}{\int_{\epsilon(\omega,t)} |\mathbf{S}(\Omega,\tau)|^2\, d\Omega\, d\tau}, \tag{7}$$

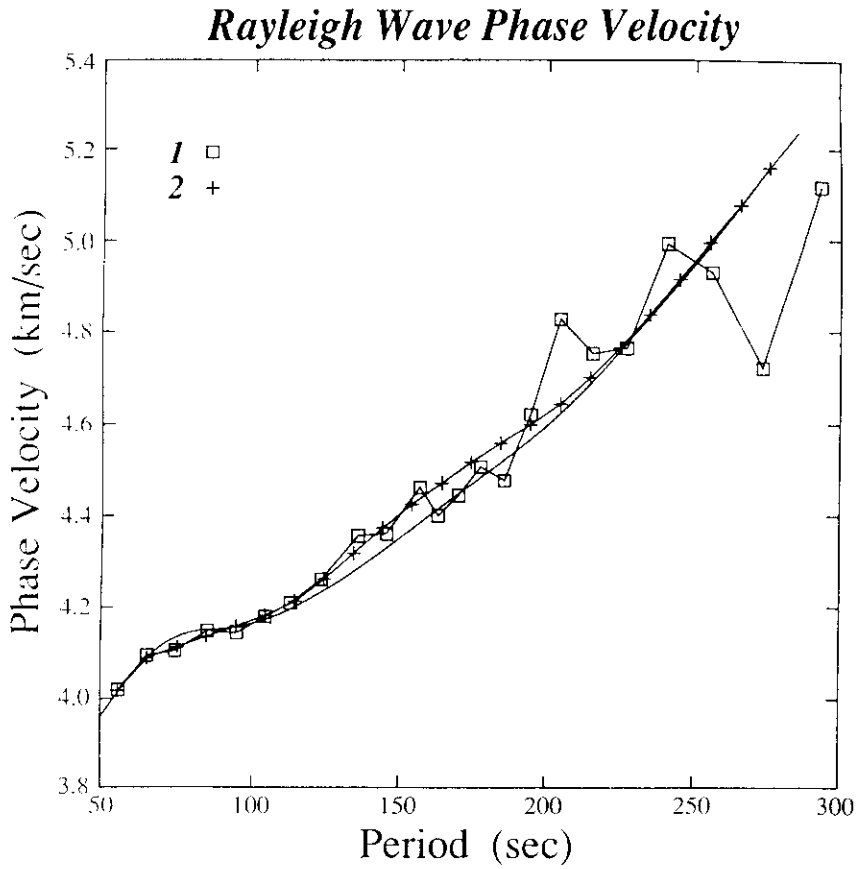

FIG. 3. Differential phase velocity measurements for the Kamchatka event of 11 April 1989 recorded at ARU and KIV. Squares: direct differential phase spectra measurements of input records; crosses: FTAN processing of input records; solid line without symbols: FTAN-processing of filtered records.

where $\epsilon(\omega, t)$ is a "scanning window," a limited region of the (ω, t) plane located around the point (ω, t). The matrix $\mathbf{C}$ is thus treated as a function defined on the frequency-time plane. By analyzing properties of the matrix $\mathbf{C}$, it is possible to estimate for each node of the grid (ω_i, t_j) the polarizational properties of this "ϵ-region," namely how close they are to Rayleigh or Love polarization. Only a few assumptions concerning each type of particle motion are made. For Rayleigh waves, predominant elliptical motion in a near-vertical plane is assumed with an vertical-to-radial ratio within some reasonable range of values, say between 0.5 and 2. For Love waves, predominantly linear near-horizontal particle motion is assumed. Thus, the "LOVE WAVE QUALITY" is defined as the product of three functions whose arguments are, respectively, the noise-to-signal ratio, the linearity of polarization, and the angle of polarization with the horizontal. The

"RAYLEIGH WAVE QUALITY" is defined as the product of three functions whose arguments are, respectively, the noise-to-signal ratio, the angle of plane of polarization with vertical, and the vertical-to radial ratio of particle motion. The "QUALITY" is close to one when noise-to-signal ratio is small and parameters of signal are close to typical one for a given wave. It drops off rapidly when a certain threshold for any of its arguments is reached. Slightly different definitions of "QUALITY" based exclusively on noise-to-signal ratio estimates were introduced by Vidale (1986) and Lerner-Lam and Park (1989).

The program produces on the screen a set of frequency-time diagrams for each type of polarization. The first of these diagrams indicates so-called "QUALITY" of signals, i.e., some relative estimate of how closely they follow our definition of a given type of polarization. The second diagram called "POWER" represents the signal power distribution in the frequency-time domain weighted by its "QUALITY." Domains of too low "QUALITY" or "POWER" are excluded from further analysis and appear as white parts of diagrams shown in this paper. The following diagrams show deviations of observed polarization from that predicted by the theory of wave propagation in laterally homogeneous isotropic media. For Rayleigh waves, they exhibit the deviation of the particle motion plane from the vertical one (called "INCLINATION") and deviation of its intersection with horizontal plane from a tangent to the great circle passing through the epicenter and the station (called "AZIMUTHAL DEVIATION"). Figure 4 serves to illustrate this terminology. For Love waves, the same terms mean deviation of predominant linear particle motion from horizontal plane and deviation of its horizontal projection from perpendicular to mentioned tangent. Other types of diagrams illustrating the signal-to-noise ratio for both types of waves and such properties of Rayleigh waves as the vertical-to-radial ratio, the tilt of the ellipse in near-vertical plane, and the direction of rotation may be produced by the program.

FTPAN also permits an estimate of average azimuthal deviation for each type of wave. This deviation is found as a mean value of azimuthal deviations for each node of the frequency-time grid weighted by its quality. Determination of these values does not depend on any *a priori* information about the epicenter position. They can be used as reliable preliminary estimates of the backazimuth

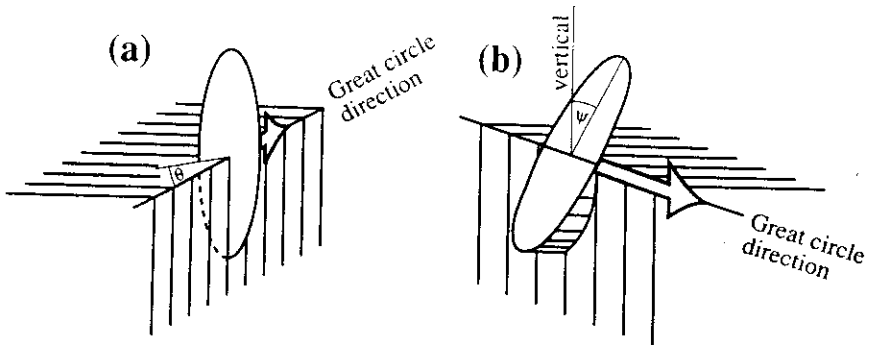

FIG. 4. Definition of angles characterizing Rayleigh-wave particle motion as estimated by polarization analysis. (a) φ: azimuthal deviation. (b) Ψ: inclination.

to an epicenter with an accuracy from 1° to 5°. In addition to diagrams, the program permits to measure all mentioned polarization parameters of the signal as a function of period. Values of parameters are determined in the frequency-time domain along the group time curve using a spline interpolation.

As the algorithm briefly described above treats the two types of surface waves independently, special care should be taken in providing sufficient resolving power to prevent Love- and Rayleigh-wave interference in time-frequency vector space. Such interference may produce drastic deterioration of "QUALITY" and/or artifacts in "AZIMUTHAL DEVIATIONS" for both types of waves, especially if very narrowband filters are used. This problem can be suppressed to some extent by a proper choice of the function $\alpha(\omega_i)$ in FTAN. Lander (personal comm.) suggested that for continental paths, the function $\alpha(\omega_i)$ constructed by the following rules:

(a) From the shortest period up to the period 60 sec, $\alpha(\omega_i)$ is taken to be optimal for the fundamental Rayleigh mode in the sense defined in Keilis-Borok

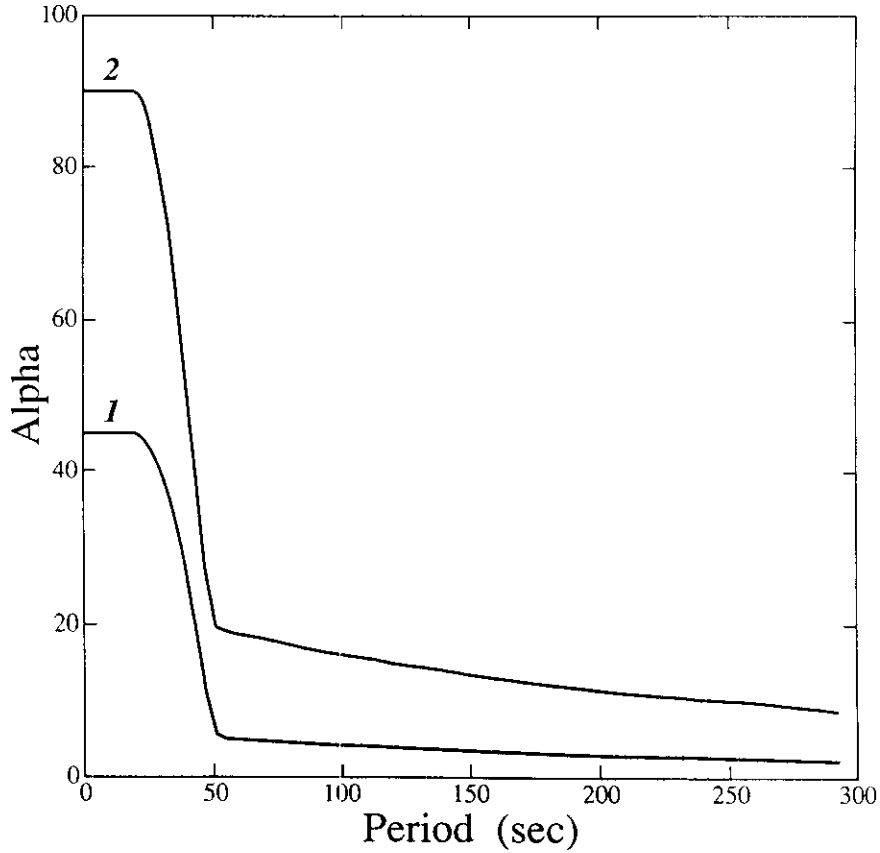

FIG. 5. Functions $\alpha(T)$ chosen for epicentral distances r = 5000 km (1) and r = 10000 km (2).

(1989):

$$\alpha_{opt}(\omega_i) = \frac{\omega_i}{2}\left|\frac{dt_{gr}(\omega)}{d\omega}\right|_{\omega=\omega_i}. \quad (8)$$

Such choice of α minimizes the area covered by this mode on a frequency-time domain.

(b) From 60 sec, $\alpha(\omega)$ is chosen to be small enough to provide the best time resolution between Love and Rayleigh fundamental modes in the range of periods where their group velocity curves are nearly flat. The functions $\alpha(T)$ obtained by these rules are shown on Figure 5. An example of such analysis is shown below for the synthetic seismogram computed for distributed source and recording station at the epicentral distance 5000 km. The Gutenberg continental model (Aki and Richards, 1980) was used to generate the fundamental Rayleigh and Love waves in the period range from 5 to 300 sec (Fig. 6a). The

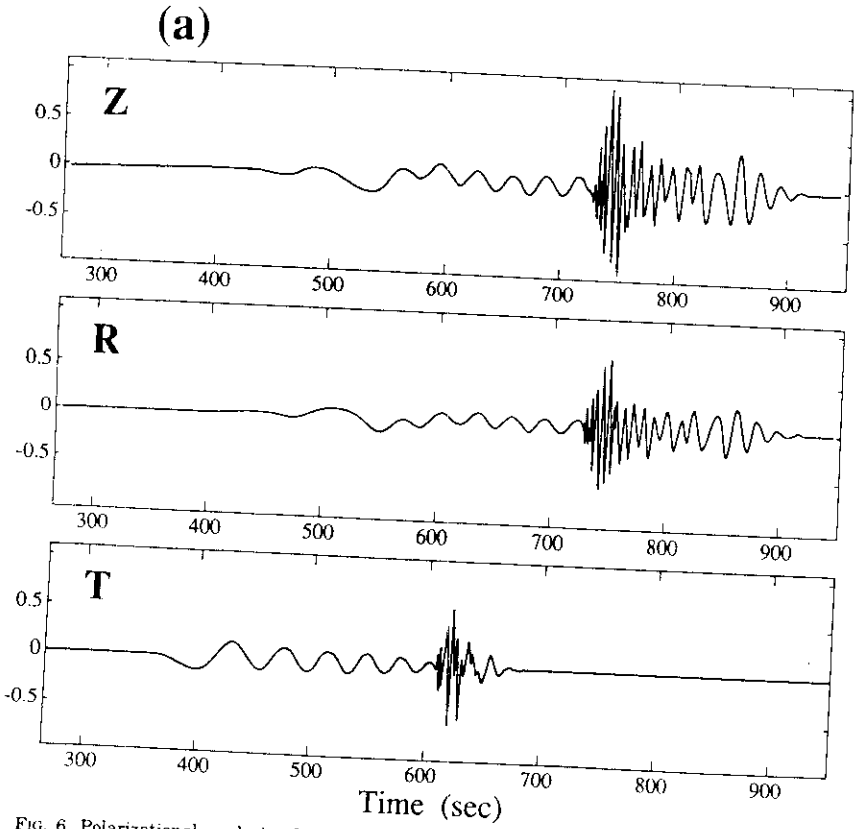

FIG. 6. Polarizational analysis of synthetic seismograms. (a) Input synthetic records, $r = 5000$ km. (b) Love-wave azimuthal deviations and energy diagram. (c) Rayleigh-wave azimuthal deviations and energy diagram.

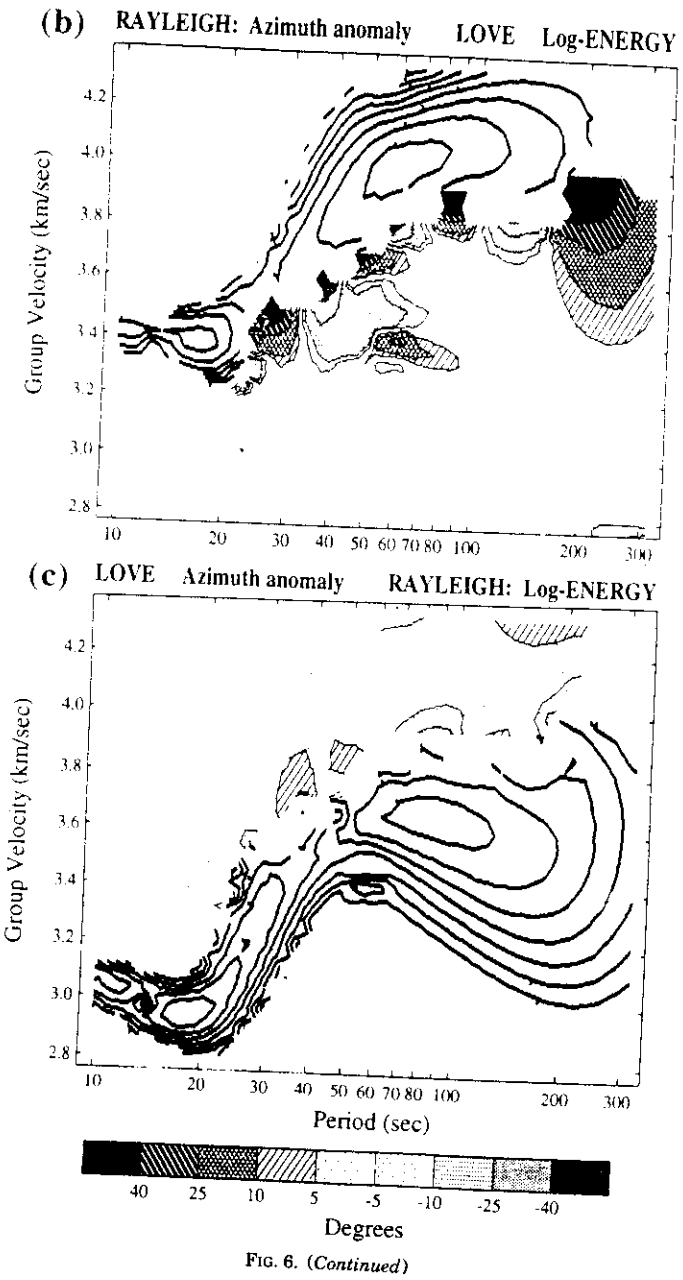

FIG. 6. (*Continued*)

source-station geometry has been chosen in this case in such a way that the maximal amplitudes of Rayleigh and Love modes were approximately the same. It is the most difficult situation for the polarization studies. Resulting polarization diagrams are shown in Figs. 7b and c. One can see that a complete resolution of two waves in a frequency-time domain at the distance around 5000 km is impossible, but outside the period range from 30 to 60 sec effects of interference are rather small. Within this range of periods, one can see strong azimuthal deviations for Rayleigh waves caused by closeness of group velocities of Love and Rayleigh waves and a small relative intensity of the Rayleigh wave at this part of spectrum. Such a low intensity is related to the particular source model, but the closeness of group velocities is rather typical. Comparison of many observed group velocity curves has shown that in this range of periods for continental paths group velocities of Rayleigh and Love waves are very close or even cross each other. Due to this fact, results of any kind of polarization analysis in this period range may be seriously biased. The best way to avoid this problem is to accept results of polarization measurements as reliable only when there are strong evidences against essential role of interference, e.g., when the wave under study is dominant on records or waves of comparable intensity are definitely resolved in the frequency-time domain. In some cases, it is possible to

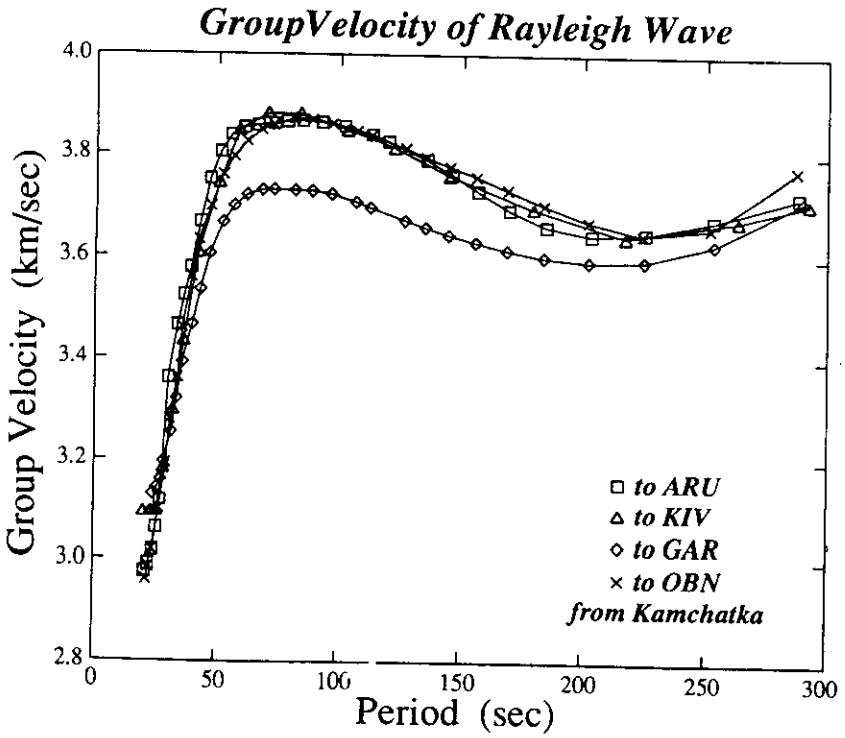

FIG. 7. Group velocity of the fundamental Rayleigh mode for paths from Kamchatka to IRIS/IDA-USSR stations.

diminish effects of interference on Rayleigh-wave analysis by subtraction of a pure Love signal, found by means of the floating filtering, from original records of horizontal instruments before processing by FTPAN.

Results of Dispersion Measurements

Group Velocities

Rayleigh-wave group velocities along paths crossing the Siberia and Russian platforms are very stable as can be seen from Figure 7. High mountain regions of central and eastern Asia are characterized by significantly lower group velocities than platforms of Siberia and western Russia. Especially low velocities of Rayleigh and Love waves were observed for paths from Southwest China to station GAR, situated at the boundary between Pamir and Tien Shan. These paths cross Tibet, the Himalayas, and the Hindu Kush-Pamir mountain systems (Fig. 8).

Phase Velocities

Only a few events were found for which epicenters were sufficiently close to the great circle passing through any pair of stations to be strong enough to be well recorded by both of them. The threshold 6° has been taken as an upper limit in azimuthal difference of two stations as seen from the epicenter. Some examples of phase measurements are shown in Figure 9.

The results obtained from clustered events are very similar (Fig. 9a), but for some pairs strong deviations of dispersion curves were obtained for waves propagating in opposite directions. An example is shown at Figure 9a for the pair KIV-OBN where dispersion curves obtained for events in Mexico and Djibouti are essentially different. This result may be explained by lateral variations of the structure crossed by waves on the way from the epicenter to the studied region. It seems that the chosen threshold in azimuthal difference should be drastically decreased, but many more data are needed to accomplish this reduction. Comparison with previous measurements of Rayleigh-wave phase velocity (Patton, 1980) that were limited by periods less than 100 sec shows reasonable agreement of results. For example, our curve for the path ARU-OBN across the Russian a platform is very close for the overlapping periods to the curve obtained by Patton for Eurasian platforms.

Observed Polarizational Properties of Surface Waves

Let us consider polarization diagrams for several strong events recorded by all four stations.

The Kamchatka Event of 11 April 1989

This event with M_s = 6.5 produced excellent records of surface waves (Figs. 10a and b). All paths are inside the continent, and, as seen from Figure 7, the group velocities of Rayleigh wave from the epicenter to stations ARU, KIV, and OBN are practically the same. Azimuths from the epicenter to KIV and ARU differ by less than 1.5°. Thus the radiation effects on Rayleigh and Love intensities should be the same for both stations.

Station OBN. This station, situated in the middle of the Russian platform, is characterized by comparatively plain relief both of the day surface and the Moho discontinuity. The epicentral distance is 7245 km and the path crosses the

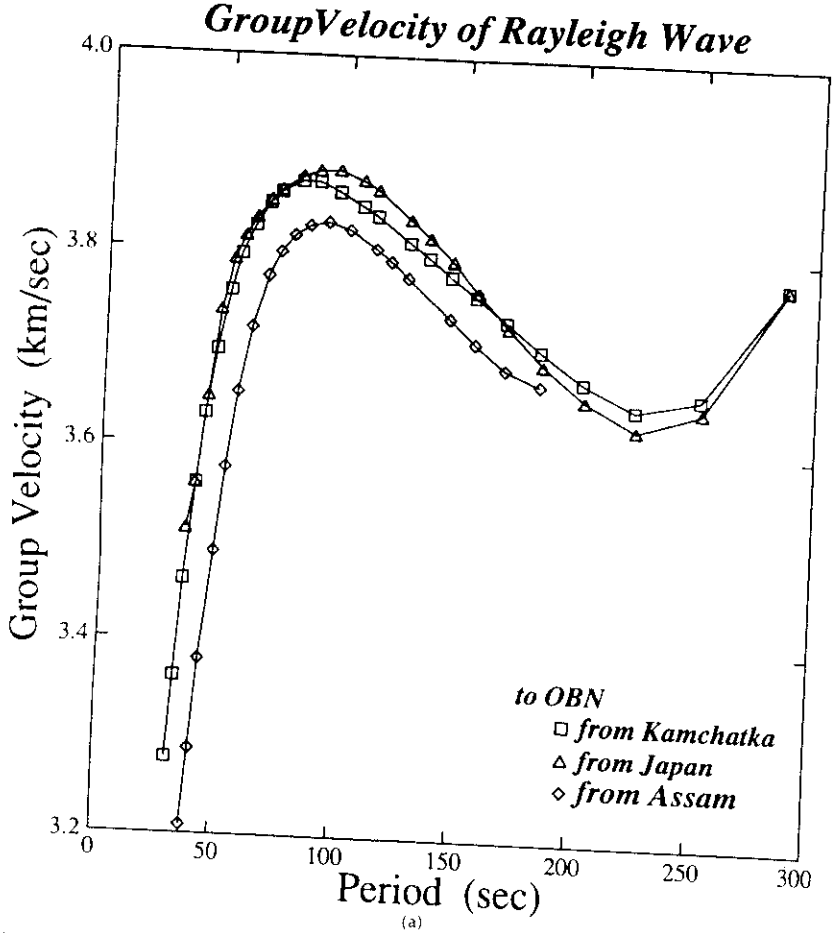

(a)

FIG. 8. Group velocity measurements. (a) Rayleigh-wave dispersion for paths to OBN from Kamchatka, Japan, and Assam. (b) Love-wave dispersion from Assam to three IRIS/IDA USSR stations.

northern part of the Sea of Okhotsk, mountains of the northeastern Siberia and the Ural, and the northern parts of the Russian and Siberian platforms. There is no strong Love wave radiated at this direction but the presence of mild interference at the beginning of the Rayleigh-wave train can be seen quite distinctly (Fig. 10c). Still we may conclude that there is no significant azimuthal deviations along the group velocity curve of the Rayleigh wave in the period range between 30 and 300 sec. At periods less than 30 sec, the patchy pattern typical for interference is predominant presumably due to the strong scattering along such a long path.

Station ARU. This station is situated at the western slope of the central Ural mountain ridge. The epicentral distance is about 6200 km and the path crosses

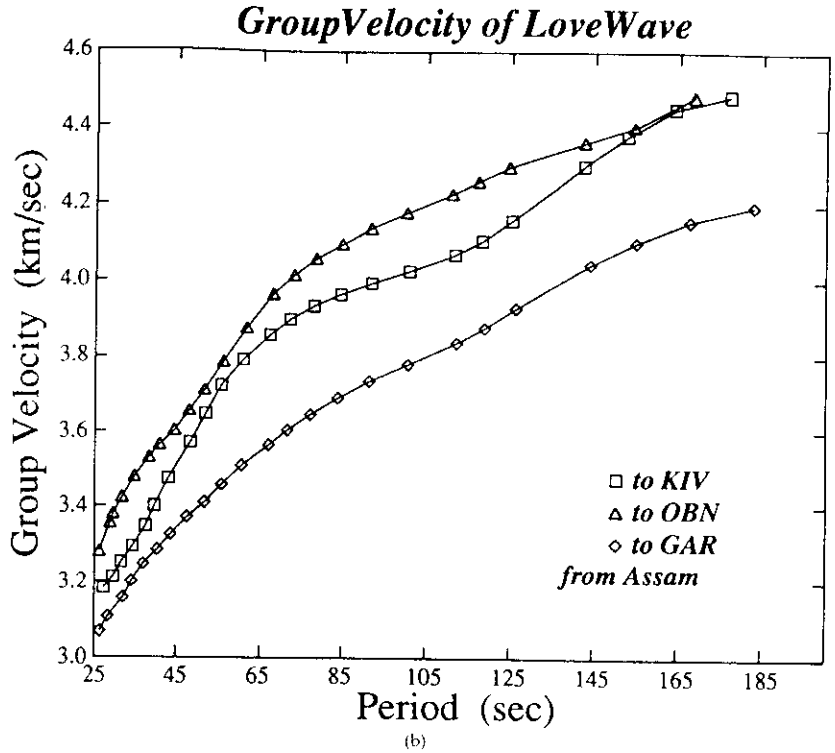

(b)

FIG. 8. (*Continued*)

the northern part of the Sea of Okhotsk, mountains of the northeastern Siberia, and the central Ural and the Siberian platform. There is no very distinct Love wave seen with periods more than 50 sec, and no azimuthal deviations of Rayleigh wave is found at this range of periods (Fig. 10d). Range between 30 and 50 sec is badly distorted by interference with the Love wave, whose group velocity curve passes very close to that of Rayleigh wave.

Station KIV. KIV is situated at the Northern slope of the Main Caucasus range quite close to Elbrus, the highest mountain in Europe. The path to the station is the same as path to ARU, except for an additional part crossing the southeast of the Russian platform including the sub-Caspian syneclise. The length of this additional part is about 1700 km. One can see a drastic decrease of amplitudes of the Rayleigh-wave train and relative increase of amplitudes of coda waves with group velocities less than 3.0 km/sec (Fig. 10e). A quite distinct azimuthal anomaly is observed for Rayleigh wave in the range of periods between 45 and 150 sec with smooth change of values from $-25°$ to $-5°$ going to zero at longer periods. This anomaly is characterized by the high "QUALITY." For shorter periods, one can see distinct interference and strong azimuthal anomalies in the coda train. There are no distinct Love waves recognized by the program.

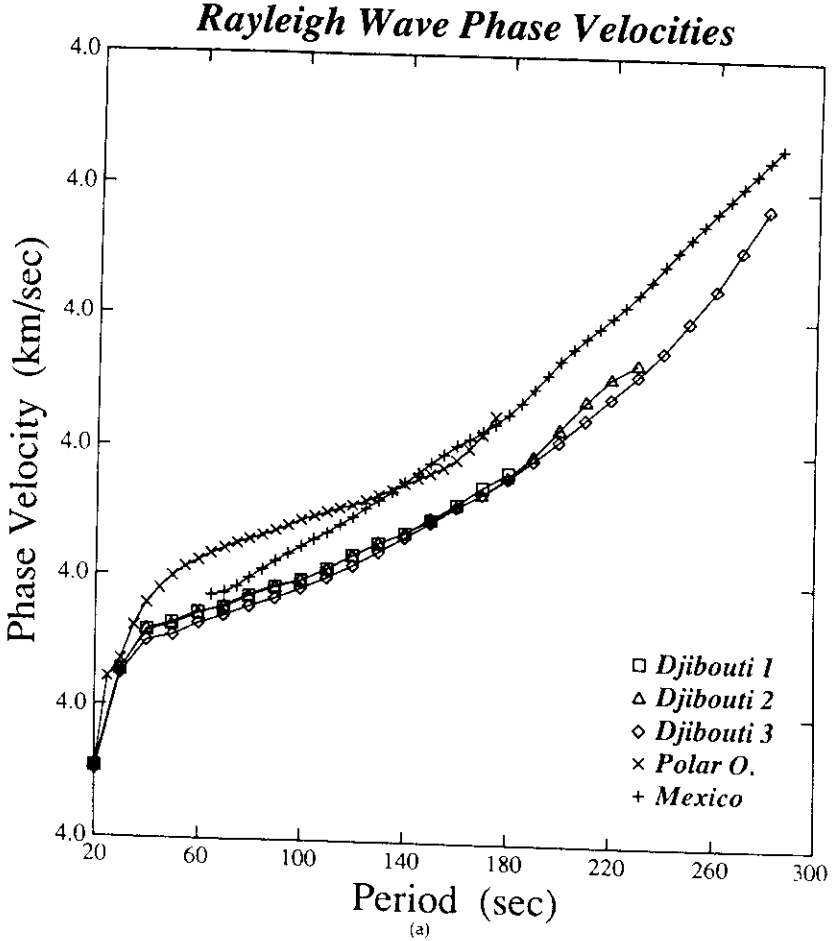

FIG. 9. Differential measurements of phase velocity for the fundamental Rayleigh mode. (a) KIV-OBN. (b) ARU-KIV. (c) KIV-GAR. (d) Selected curves for five pairs of stations.

Station GAR. this station is situated in the tectonic region between Tien Shan and Pamir mountains. The path is 6770-km long and crosses mountain regions of the eastern Siberia, Altai, Sayan, and Tien Shan mountains. Both Love and Rayleigh fundamental modes are recorded in a wide range of periods. No anomaly is observed for the Rayleigh mode for periods between 60 and 120 sec, but for shorter periods between 40 and 60 sec there is a quite distinct negative anomaly (Fig. 10f). It has about the same magnitude from $-20°$ to $-15°$, as seen at Figure 10g for the Love wave in the period range between 40 and 120 sec. The "QUALITY" of Love wave in this period range is high. Group velocities of both waves along this path are not too close in the whole period range.

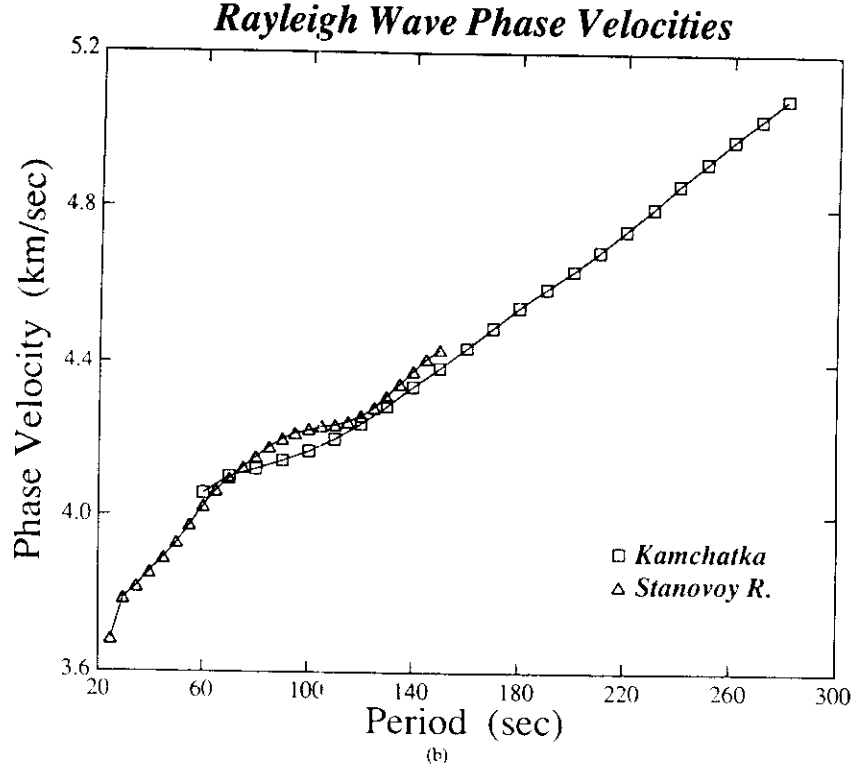

FIG. 9. (*Continued*)

The Philippines Event of 16 July 1990

This is a strong event (M_s = 7.8) for which all stations lie in the narrow azimuthal window between 307° and 326°. All paths to stations cross the South China Sea and the plains of southern China. A strong fundamental Love mode is dominant on all records (Fig. 11a). The fundamental Rayleigh mode is hardly seen except short-period bursts of energy at low group velocities not shown here.

Station OBN. The path to OBN crosses also northeastern Tibet, eastern Tien Shan, the Kazakh folded country, and the Siberian and Russian platforms. There is no significant azimuthal deviations of the Love wave in the whole range of periods between 25 and 200 sec (Fig. 11b).

Station ARU. The path from the epicenter goes slightly more to the North than in the case of OBN and avoids the Tibetan plateau. There is no anomalies of Love-wave polarization except for periods between 30 and 40 sec where interference with a relatively more strong Rayleigh wave is possible due to the shorter epicentral distance (Fig. 11c).

Station KIV. The path crosses the Tibetan plateau at its central part, the Tarim platform, the western Tien Shan, and the Turan and Scythean platforms.

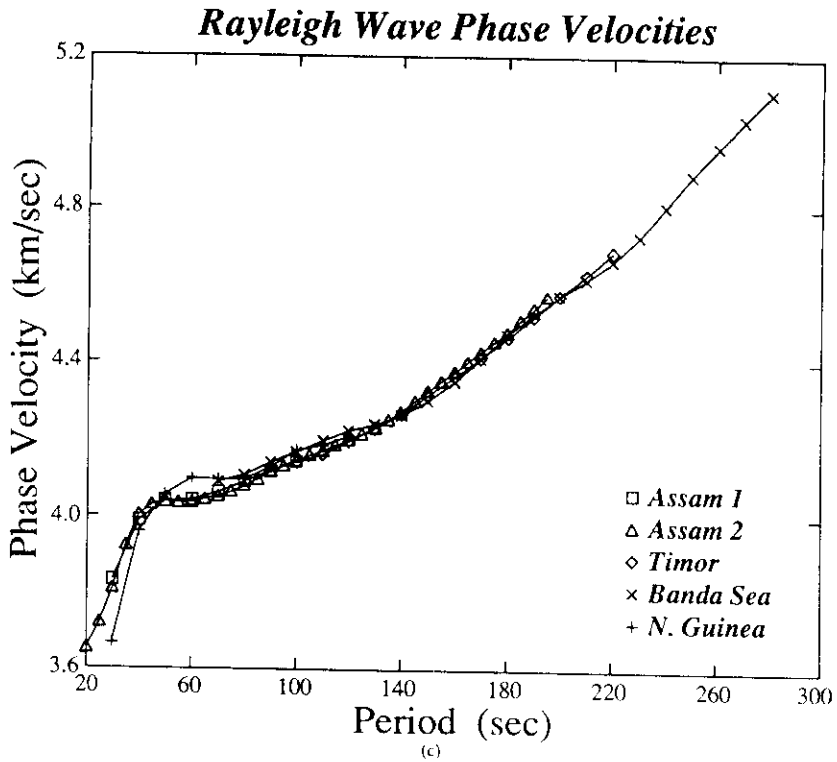

(c)

FIG. 9. (*Continued*)

Strong azimuthal anomaly of the Love wave is observed decreasing from $-20°$ at the period about 30 sec to $-10°$ at 200 sec (Fig. 11d).

Station GAR

The path crosses central Tibet, Karakorum, Hindu Kush, and Pamir. There are no strong azimuthal deviations observed for the Love wave except a mild anomaly in the range of 50 to 80 sec with values of deviation around $-7°$ (Fig. 11e).

Stability of Polarization Diagrams

As the patterns of polarization described above seem to be rather complicated, the stability in polarization diagrams was checked for a set of seismograms generated by clustered events. Similar polarization patterns both for Love and Rayleigh waves generated by such events were found.

Azimuthal Dependence of Polarization Anomalies

It is interesting to see if there is a dependence of observed anomalies on the azimuth of approach to stations. Selected data permit at least a preliminary estimate of such effects for OBN and KIV.

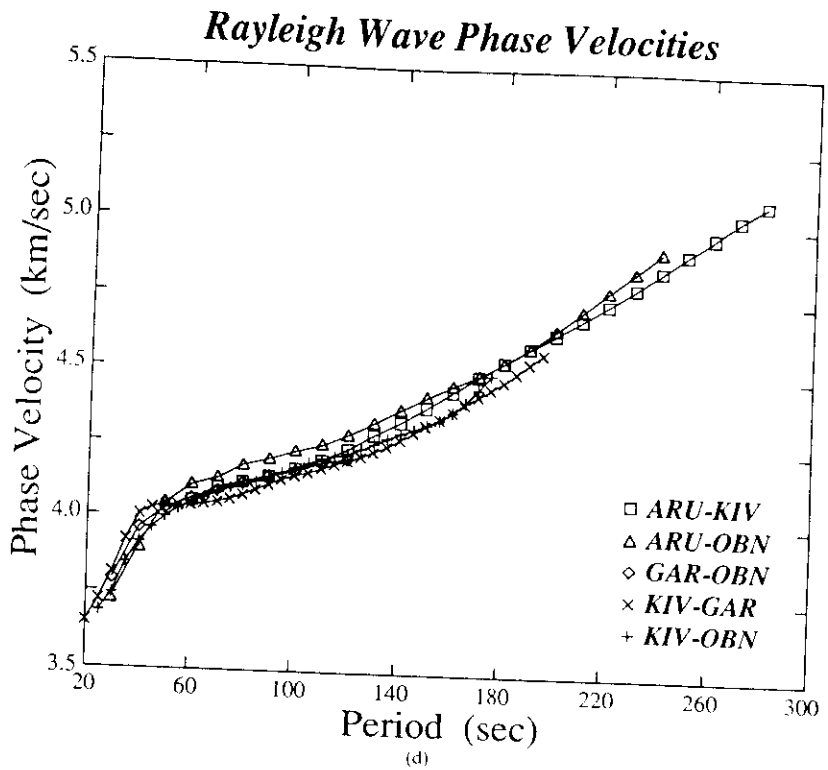

(d)

FIG. 9. (*Continued*)

Station OBN. No significant anomalies was found for Love waves with periods more than 40 sec coming from the northwest (Norwegian Sea), the north (Mexico and northern California), the east (Stanovoy Range, Honsu, Philippines), or the south (Djibouti). Only in some cases are mild anomalies observed for the period range between 50 and 80 sec for earthquakes at the Marian Trench and near Timor. Some deviations observed at short-period Rayleigh waves can be explained by interference with Love waves, especially for not-too-distant events such as that at the Norwegian Sea on 9 June 1989. At the same time, we think that some of observed short-period deviations are real azimuthal anomalies due to the propagation conditions on the path from an epicenter to the station.

Station KIV. No significant deviations are observed for waves coming from the north (Mexico) or from the south (Djibouti) for periods more than 50 sec. Shorter periods exibit significant deviations whose sign may change with period. Waves coming from events at the east and the southeast are characterized by stable negative azimuthal deviations for periods between 40 and 100 sec, the values of deviation varying from $-15°$ to $-5°$.

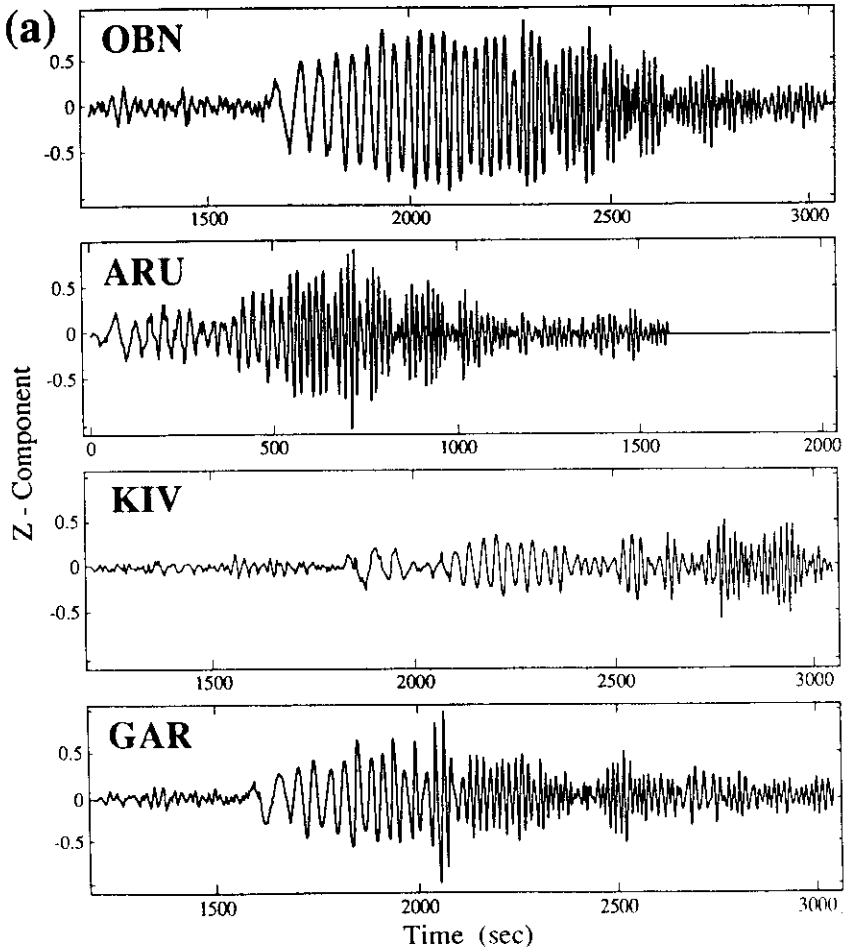

FIG. 10. (a) Vertical and (b) transverse components of seismograms and azimuthal deviations the particle motion for the Kamchatka event of 11 April 1989 at (c) stations OBN, (d) ARU, (e) KIV, (f and g) GAR. This solid line shows the position of the energy maximum as a function of period.

DISCUSSION

There are several possible reasons for deviation of particle motion planes from the theoretical one for the spherically symmetrical isotropic Earth. Let us mention and discuss them.

Instrumental Errors such as Wrong Calibration and Inaccurate Azimuthal Orientation. They can be rejected, as in many cases no any anomaly of polarization was observed at given station and average backazimuths differ from theoretical by less than 1°.

Interference of Regular Waves Having Different Polarization, e.g., of Different

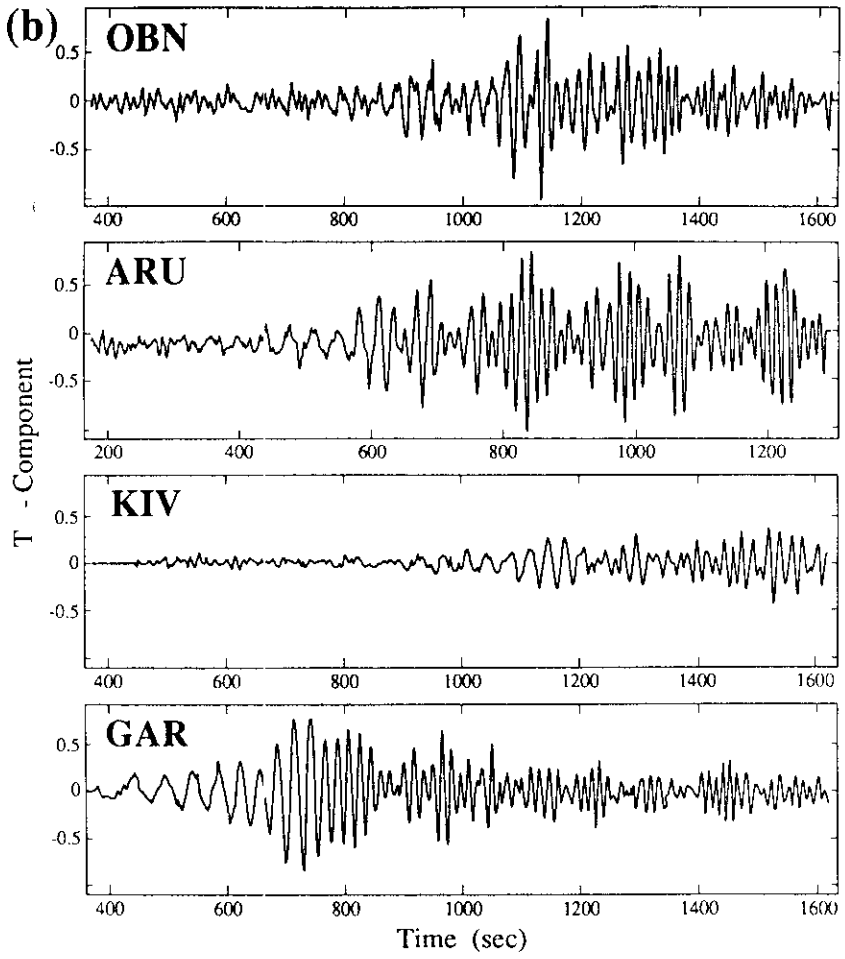

FIG. 10. (*Continued*)

Modes of Rayleigh and Love Waves. This is a quite common case especially in the range of periods between 30 and 50 sec and group velocities between 3.6 and 3.8 km/sec. In this time-frequency region, the group velocities of two fundamental modes are very close. Rayleigh-wave polarization could be especially strongly affected, due to the fact that in some time-frequency zones orthogonal horizontal components of both waves may be almost in phase or in anti-phase. Inside such a zone, the Rayleigh-wave polarization is accepted by the program with the high levels of "QUALITY" and "POWER" but with a significant azimuthal deviation. Other problematic regions are for periods between 50 and 70 sec and group velocities between 4.1 and 4.3 km/sec, where group velocities of the fundamental Love mode and the first higher mode of the Rayleigh wave

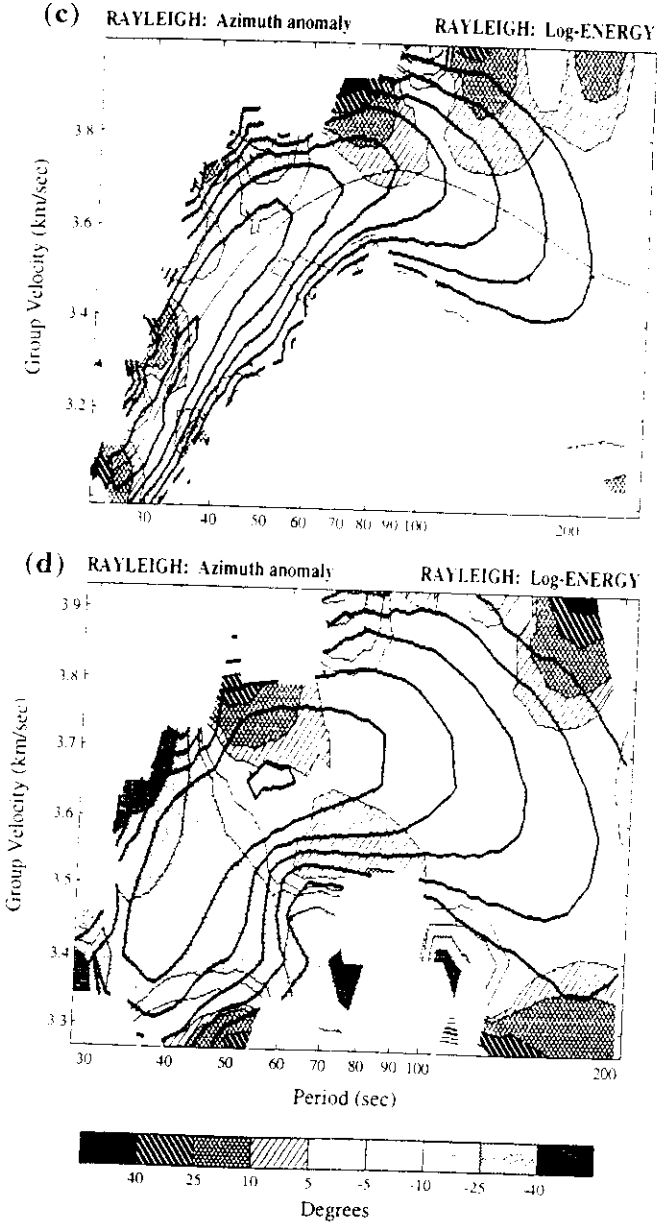

FIG. 10. (*Continued*)

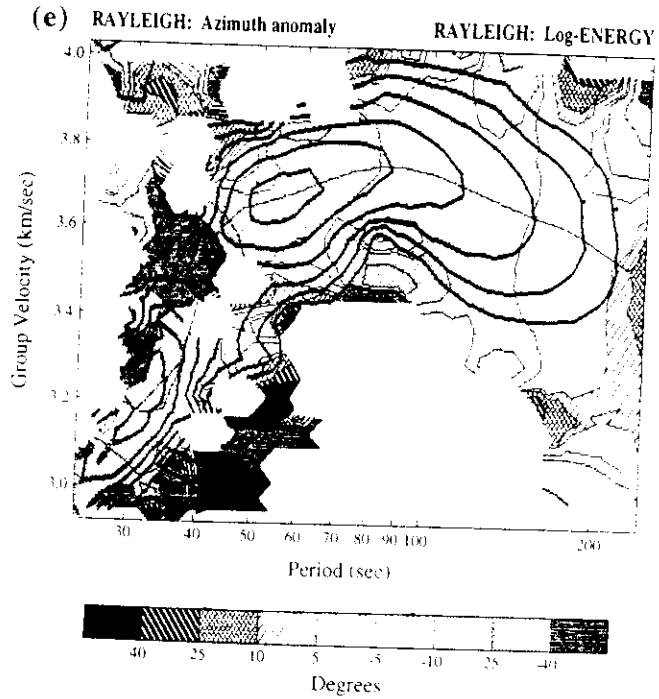

FIG. 10. (*Continued*)

are quite close. Fortunately in many cases the higher mode is not strong enough to disturb the Love-wave polarization diagrams. Nevertheless, significant distortions of Love-wave polarizations observed sometimes in this time-frequency region may be explained by this effect. Still, in many cases, we see on records only one strong surface wave, and observed anomalies cannot be explained by this way.

Interference of the Wave under Study with Scattered Fields of Preceding or Following Waves, e.g., Love-to-Rayleigh Backward Scattered Field or Rayleigh-to-Love Forward Scattered Fields. It seems that in the direction of propagation such scattered fields are relatively weak (Snieder, 1986), but for distant events such phenomena are definitely present due to complicated wave paths at periods less than say 30 to 40 sec. It is difficult to explain by the reason significant anomalies observed for wide range of periods as shown at Figures 10d to f or Figures 11d and e.

Local Effects of the Structure near the Station. This should be important for such stations as KIV or GAR situated near or inside high mountain regions at comparatively short periods. Many more data are needed for detailed study of these effects.

Anisotropic Properties of the Crust or the Lithosphere in Whole. The behavior of surface waves in anisotropic models of the Earth was studied by Crampin (1975, 1981). From his study, it seems that significant effects of anisotropy on

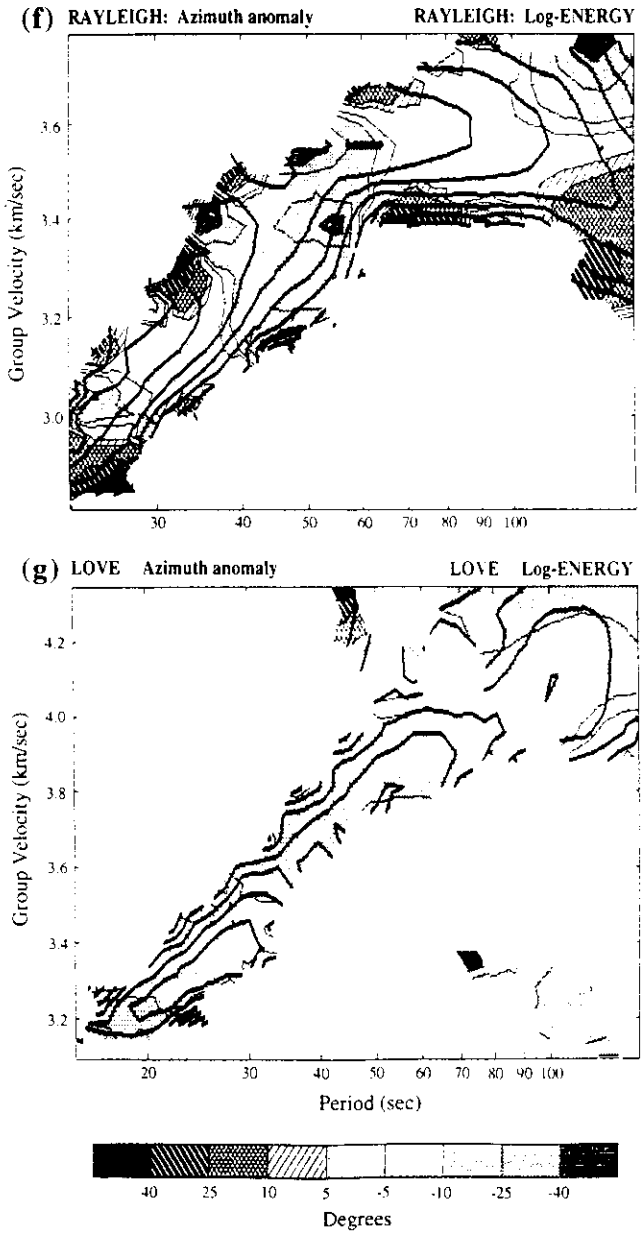

FIG. 10. (*Continued*)

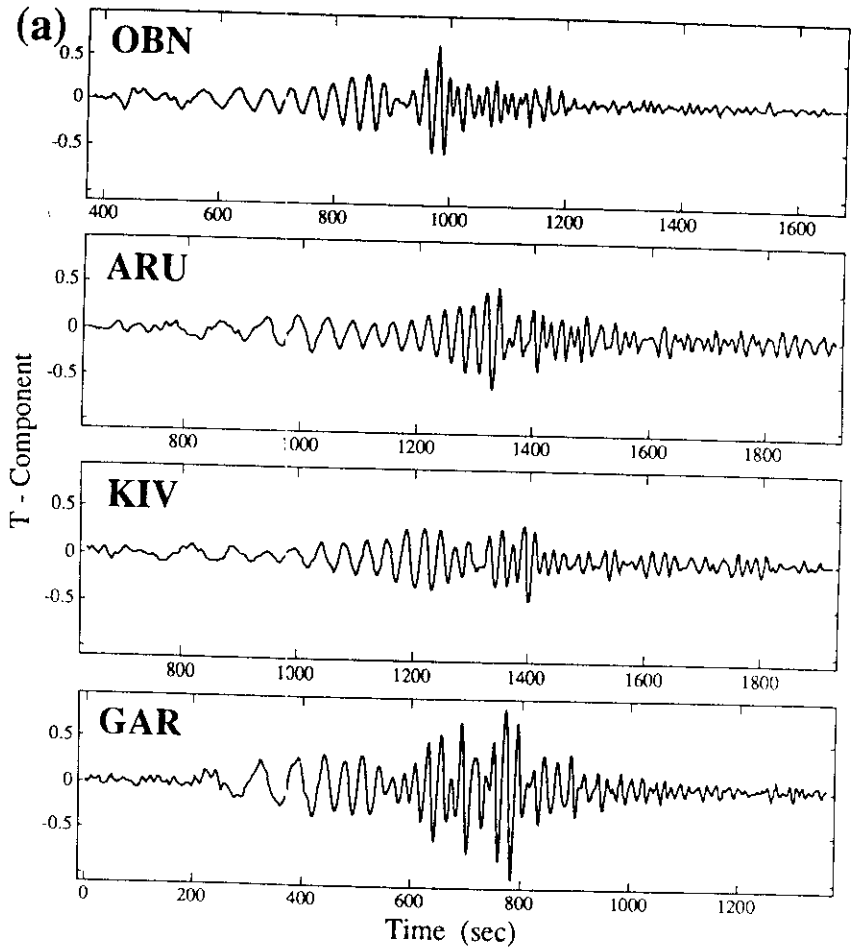

FIG. 11. Transverse components of seismograms and azimuthal deviations of the particle motion for the Philippines event of 16 July 1990 at (b) stations OBN, (c) ARU, (d) KIV, (e) GAR.

particle motion should appear at higher modes but are practically negligible for two lowest modes, which correspond to fundamental Love and Rayleigh modes in isotropic models. It is necessary to mention that calculations were done by Crampin for the continental Earth structure having a thin layer of a comparatively weak orthorombical anisotropy in the upper mantle with a horizontal plane of symmetry. Stronger anisotropy of the same kind may produce more significant effects even on lowest modes, which ought to appear as consistent deviations and inclinations of the particle motion plane. They should depend on azimuth of approach by a regular way. In our case, no regular azimuthal dependence of polarization anomalies was observed. However, this result does

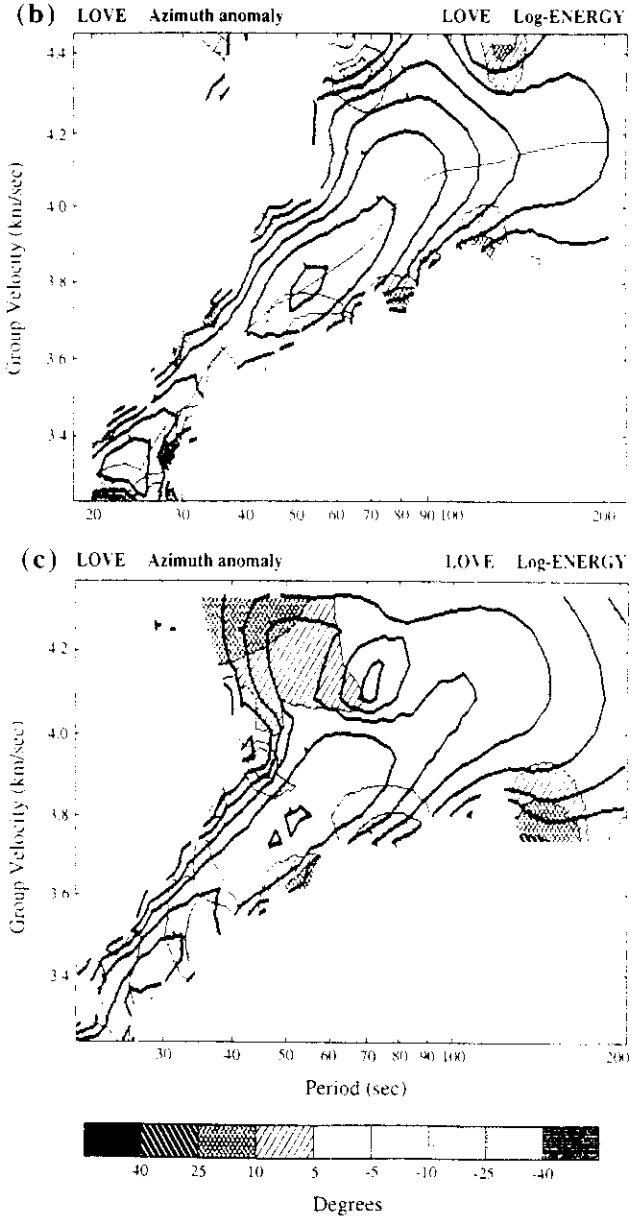

FIG. 11. (*Continued*)

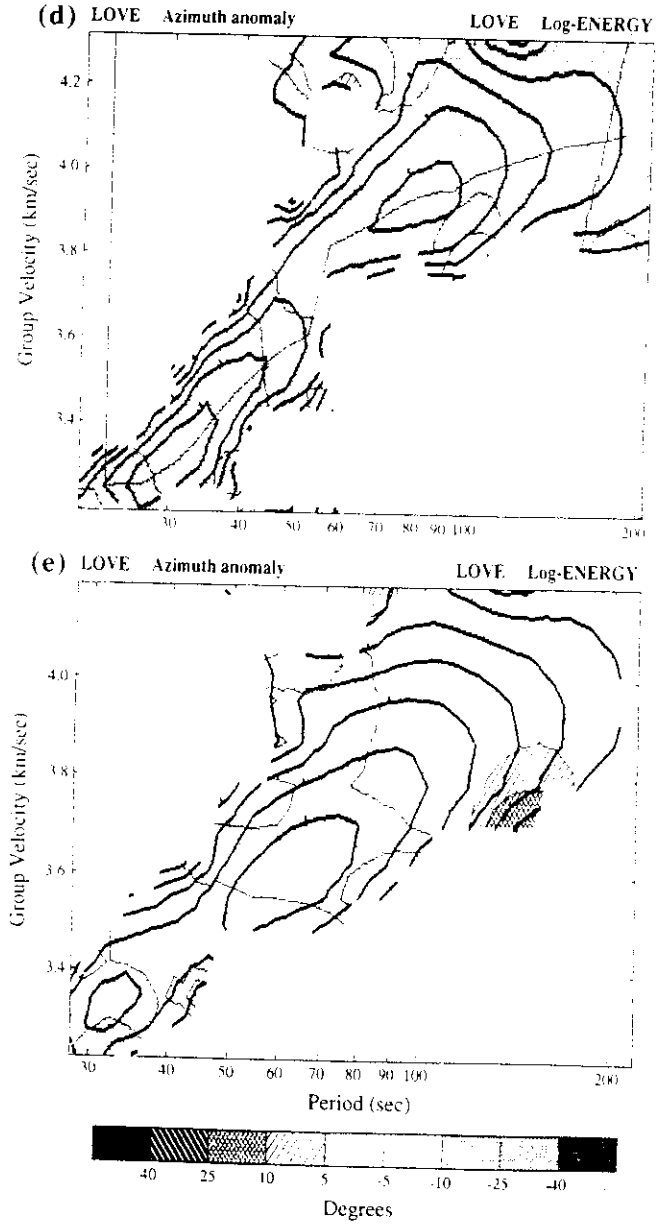

FIG. 11. (*Continued*)

not rule out the presence of anisotropy in the crust and mantle as one of factors influencing particle motion.

Refraction of Surface Waves by Lateral Inhomogeneities along the Path between Source and Station (Patton, 1980; Jobert and Jobert, 1983; Woodhouse and Wong, 1986; Yomogida and Aki, 1987; Keilis-Borok, 1989; Lerner-Lam and Park, 1989). This seems to us to be the most plausible explanation of observed deviations, especially in the long-period part of wave spectra. Azimuthal anomalies observed at the stations KIV and GAR for paths from the east are predominantly negative. It can be interpreted in such a way that actual wave paths follow along faster trajectories and deviate to the north from great circle paths. Great circle paths to KIV from the east and the northeast are crossing the sub-Caspian syneclise—one of the greatest sedimentary basin of the world. Previous studies demonstrated very low phase velocities of Rayleigh waves with periods less than 30 to 40 sec along this basin (Levshin *et al.*, 1982). The deviation of wave paths to the north makes the possibility of avoiding this basin and observed azimuthal anomalies for short-period waves seem natural. A strong attenuation of the Rayleigh wave between ARU and KIV and a relative growth of coda amplitudes at KIV could be also attributed to the effect of this basin. Observed anomalies for longer periods can be explained by a general increase of upper-mantle velocities at the direction from the Scythean and Turan platforms to the Siberian and Russian platforms as indicated by DDS data (Volvovsky and Volvovsky, 1975) and surface-wave studies (Patton, 1980). Observed anomalies at GAR can be explained by similar reasons. The great circle path from Kamchatka crossing different mountain regions of Siberia and central Asia is definitely slower than paths deviating to the north to follow along the Siberian platform with thinner crust and higher upper-mantle velocities (Patton, 1980; Kozhevnikov, 1987; Kozhevnikov and Barmin, 1989). More southern paths to GAR from southern Japan and the Philippines tend to deviate to the north to avoid the Tibetan plateau with its very thick crust.

Conclusions

Recent deployment of the IRIS/IDA broadband digital network in the USSR has opened new opportunities for studies of surface-wave propagation across central Eurasia with implications for recovering lateral inhomogeneities of the crustal and upper-mantle structure in this huge continental territory. In parallel with traditional dispersion measurements, a new technique of the frequency-time polarization analysis was applied for investigation of surface-wave polarization properties. Detailed analysis of the limited amount of accumulated data clearly demonstrates such effects of lateral inhomogeneities on surface-wave propagation as difference in two-station phase velocities for waves traveling in opposite directions and significant particle motion anomalies in a wide range of periods. These anomalies are qualitatively explained by regional differences of the lithosperic structure. A longer period of observations is necessary to give a quantitative interpretation of observed effects and provide tomographic inversion. Data from newly installed stations in Armenia, Kirgizia, and near Lake Baikal would be important additional contribution to this kind of study.

Acknowledgments

This research has been started when one of authors (A. L.) was a Cecil H. and Ida M. Green Scholar at the Institute of Geophysics and Planetary Physics, Scripps Institution of Oceanography. He gratefully acknowledges this support. We wish to thank Dr. A. Lander for making available his computer program for the polarizational analysis and many useful suggestions, Drs. H. Given, D. Chavez, F. Vernon, and A. Egorkin for their kind help in the data analysis and graphic representation of results.

References

Aki, K. and P. G. Richards (1980). *Quantitative Seismology*, vol. 1, W. H. Freeman, San Francisco.

Alekseev, A. S., A. V. Belonosova, G. V. Krasnopevtseva, N. N. Matveeva, I. L. Nersesov, N. I. Pavlenkova, V. G. Romanov, and V. Z. Ryaboy (1973). Seismic studies of low-velocity layers and horizontal inhomogeneities within the crust and upper mantle on the territory of USSR, *Tectonophysics* **20,** 47–56.

Atonenko, A. N. (1984). Deep crustal structure of Kazakhstan from seismic data, *Alma-Ata, Nauka*, (in Russian).

Barmin, M. P., S. E. Kapitanova, A. L. Levshin, S. B. Nikolova, T. M. Sabitova, O. E. Starovoit, and T. B. Yanovskaya (1984). Investigations of lateral inhomogeneities of the lithosphere by surface waves, in *Present State of seismological studies in Europe: Proceedings of XIX Assembly of ESC*, Nauka, Moscow, 428–439 (in Russian).

Belyaevsky, N. A., B. S. Volvovsky, I. S. Volvovsky, *et al.*, (1977). Seismic crustal structure of Eastern Europe, in *Crustal and Upper Mantle Structure from Seismic Observations*, Naukova Dumka, Kiev, 4–19 (in Russian).

Bougaevskii, G. N. (1978). *Seismological Investigations of Inhomogeneities of the Earth's Mantle*, Kiev, Naukova Dumka (in Russian).

Cara, M. (1973). Filtering of dispersed wave trains, *Geophys. J. R. Astr. Soc.* **33,** 65–80.

Chang, F. (1979). The structure of the upper mantle of Eurasia and tectonic interpretation from a study of Rayleigh wave dispersion, *Ph.D. Thesis*, UCLA, Los Angeles.

Crampin, S. (1975). Distinctive particle motion of surface waves as a diagnostic of anisotropic layering, Geophy. J. R. Astr. Soc. **40,** 177–186.

Crampin, S. (1981). A review of wave motion in anisotropic and cracked elastic-media, *Wave Motion* **3,** 343–391.

Dziewonski, A. M., S. Bloch, and M. Landisman (1969). A technique for the analysis of transient seismic signals, *Bull. Seism. Soc. Am.* **59,** 427–444.

Dziewonski, A. M., J. Mills, and S. Bloch (1972). Residual dispersion measurement: a new method of surface wave analysis, *Bull. Seism. Soc. Am.* **62,** 129–139.

Egorkin, A. V. and N. I. Pavlenkova (1981). Studies of mantle structure of the USSR territory on the long-range seismic profiles, *Phys. Earth. Planet. Interiors* **25,** 12–26.

Egorkin, A. V., S. K. Ziuganov, and N. M. Chernyshov (1984). The upper mantle of Siberia, in *Proc. 27th Int. Geological Congress*, Vol. 8, Geophysics, Nauka, Moscow, 27–42 (in Russian).

Given, H. (1990). Variations in broadband seismic noise at IRIS/IDA stations in the USSR with implications for event detection, *Bull. Seism. Soc. Am.* **80,** 2072–2080.

Jobert, N. and G. Jobert (1983). An application of ray theory to the propagation of waves along a laterally heterogeneous spherical surface, *Geophys. Res. Lett.* **10,** 1148–1151.

Keilis-Borok, V. I. (Editor) (1989). *Seismic Surface Waves in Laterally Inhomogeneous Earth*, Kluwer Dordrecht. (Originally 1986, Nauka, Moscow, in Russian.)

Knopoff, L. and F. Chang (1976). The Rayleigh wave propagation in a regionalization of Eurasian Continent (abstract), *Earthquake Notes* **47,** no. 2, 5.

Kozhevnikov, V. M. (1987). Dispersion of surface Rayleigh waves and the structure of the Siberian plate lithosphere, *Izvestia Fizika Zemli* **6,** 48–56.

Kozhevnikov, V. M. and M. P. Barmin (1989). Rayleigh wave group velocity dispersion curves for several regions of Eurasian continent, *Izvestia Fizika Zemli* **9,** 16–25.

Lander, A. V. and A. L. Levshin (1982). Azimuthal and polarization anomalies of surface waves and the methods for studying them, in *Development of G. A. Gamburtsev's Ideas in Geophysics*, Nauka, Moscow, 248–260 (in Russian).

Lerner-Lam, A. L. and J. J. Park (1989). Frequency-dependent refraction and multipathing of 10–100 second surface waves in the western Pacific, *Geophys. Res. Lett.* **16,** 527–530.

Levshin, A. L., V. F. Pisarenko, and G. A. Pogrebinsky (1972). On a frequency-time analysis of oscillations, *Ann. Geophys.* **28,** 211–218.

Levshin, A. L., L. I. Ratnikova, and K. A. Berteussen (1982). Regional studies of Eurasian crust using surface waves, in *Mathematical Earth Models and Earthquake Prediction*, Nauka, Moscow, 105–117 (in Russian).

Liao, A. H. (1981). Anisotropy in the upper mantle of Eurasia, *Ph.D. Thesis*, UCLA, Los Angeles.
Louck, A. A. and I. L. Nersesov (1965). The structure of upper mantel from the observations of earthquakes with intermediate source depth, *Proc. Acad. Sci. USSR* **162** (in Russian).
Nolet, G. (Editor) (1987). *Seismic Tomography*, Kluwer, Dordrecht.
Patton, H. (1980). Curst and upper mantle structure of the Eurasian continent from the phase velocity and Q of surface waves, *Rev. Geophys. Space Phys.* **18,** 605–625.
Paulssen, H., A. L. Levshin, A. V. Lander, and R. Snieder (1990). Time- and frequency-dependent polarization analysis: anomalous surface wave observations in Iberia, *Geophys. J. Int.* **103,** 483–496.
Pavlenkova, N. I. and A. V. Egorkin (1983). Upper mantle heterogeneity in the northern part of Eurasia, *Phys. Earth. Planet. Interiors* **33,** 180–193.
Ryaboy, V. Z. (1979). *The Upper Mantle Structure of the USSR Territory from Seismic Data*, Nedra, Moscow (in Russian).
Snieder, R. (1986). 3-D linearized scattering of surface waves and a formalism for surface wave holography, *Geophys. J. R. Astr. Soc.* **84,** 581–605.
Vidale, J. E. (1986). Complex polarization analysis of particle motion, *Bull. Seism. Soc. Am.* **76,** 1393–1405.
Vinnik, L. P. and A. V. Egorkin (1980). Wave fields and models of litosphere and astenosphere from the seismic observation data in Siberia, *Proc. Acad. Sci. USSR* **250,** 2 (in Russian).
Vinnik, L. P. and V. Z. Ryaboy (1981). Deep structure of the East European platform according to seismic data, *Phys. Earth Planet. Interiors* **25,** 27–37.
Volvovsky, I. S. and B. S. Volvovsky (1975). *Crustal Cross-Sections of the Territory of the USSR from Deep Seismic Sounding Data*, Sov. Radio, Moscow (in Russian).
Woodhouse, J. H. and Y. K. Wong (1986). Amplitude, phase and path anomalies of mantle waves, *Geophys. J. R. Astr. Soc.* **87,** 753–773.
Yanovskaya, T. B. and S. B. Nikolova (1984). Distribution of Rayleigh and Love surface wave group velocities in Southeastern Europe and Asia Minor, *Geofiz. Zhurn. Bolg. AN* **10,** no. 4, 83–92 (in Russian).
Yomogida, K. and K. Aki (1987). Amplitude and phase data inversions for phase velocity anomalies in the Pacific Ocean basin, *Geophys. J. R. Astr. Soc.* **88,** 161–204.
Zunnunov, F. H. (1985). *The Lithosphere of Central Asia from Seismic Data*, FAN Uzbek SSR. Tashkent (in Russian).
Zverev, S. M. and I. P. Kosminskaya (Editors) (1980). *Seismic Models of the Main Geostructures of USSR Territory*. Nauka, Moscow (in Russian).

INTERNATIONAL INSTITUTE
OF EARTHQUAKE PREDICTION
THEORY AND MATHEMATICAL GEOPHYSICS
RUSSIAN ACADEMY OF SCIENCES
(A.L., L.R.)

INSTITUTE OF GEOPHYSICS AND PLANETARY PHYSICS
SCRIPPS INSTITUTION OF OCEANOGRAPHY (A025)
UNIVERSITY OF CALIFORNIA SAN DIEGO
LA JOLLA, CALIFORNIA 92093-0225
(J.B.)

Manuscript received 20 September 1991